Annals of Phytomedicine 12(1): 269-276, 2023

DOI: http://dx.doi.org/10.54085/ap.2023.12.1.2

Annals of Phytomedicine: An International Journal

http://www.ukaazpublications.com/publications/index.php

Print ISSN : 2278-9839 Online ISSN : 2393-9885

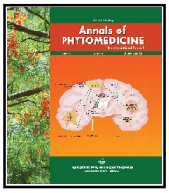

Original Article : Open Access

Computational identification of bioactive compound with neuroprotective potential for the management of Alzheimer's disease by targeting AChE protein

Firdaus Jahan, Akanksha Sharma* and Mohammad Hayatul Islam◆

IIRC-5, Clinical Biochemistry and Natural Product Research Lab, Department of Biosciences, Faculty of Science, Integral University, Lucknow-226010, Uttar Pradesh, India

** Department of Biotechnology, SR Group of Institute, Sitapur Road, Bakshi Ka Talab, Lucknow-226201, Uttar Pradesh, India*

Article Info

Article history

Received 12 January 2023

Revised 10 March 2023

Accepted 11 March 2023

Published Online 30 June-2023

Keywords

Secondary metabolites

Alzheimer's disease

Molecular docking

Binding energy

Molecular dynamics simulation

Abstract

Alzheimer's disease (AD) is a progressive neurodegenerative disease (ND) and the most prevalent cause of dementia. Acetylcholinesterase (AChE) is the primary cholinesterase responsible for catalyzing the breakdown of acetylcholine and other choline esters that function as neurotransmitters in the body. Given that Alzheimer's disease is a neurological disorder, AChE is thought to play a crucial role in its pathogenesis. On the basis of available literature from neuroprotective plants, a list of 100 secondary metabolites has been compiled. Out of 100 compounds, only forty have drug like properties, and out of these ten, only four satisfy the ADMET criteria. These four are docked against the AChE receptor and validated using redock docking. Kanzonol R (Isoflavonoid) showed significant binding affinity with a binding energy of –10.67 kcal/mol as compared to the redock complex. Kanzonol R has the highest binding affinity and is thus subjected to a complex stability study using molecular dynamics over 100 ns. Kanzonol R outperformed the other compounds and the redock crystal structure in terms of binding affinity and structure stability. The MM-PBSA analysis also shows Kanzonol R and AChE having stable interactions throughout the 100 ns trajectory, and therefore, Kanzonol R may be used as a potent inhibitor of AChE in AD management.

1. Introduction

In the process known as neurodegeneration, the progressive loss of a neuron's structure or function results in neurodegenerative diseases. Cell death may eventually result from such neuronal damage. Neurodegenerative diseases are crippling, incurable conditions that cause nerve cells to gradually deteriorate and die (Huang *et al*., 2020, Davenport *et al*., 2023). Huntington, Alzheimer, and Parkinson diseases, along with conditions like amyotrophic lateral sclerosis and multiple sclerosis, are examples of neurodegenerative conditions. The most prevalent neurodegenerative illnesses are Parkinson's and Alzheimer's diseases (AD). The consequences of AD often manifest later in life, and at 65 years of age, its frequency generally doubles every 5 years (Marucci *et al*., 2021).

Furthermore, as life expectancy rises, so does the prevalence of AD and other age-related disorders. AD is by far the most prevalent kind of dementia (Poddar *et al*., 2021), accounting for roughly 70-80% of cases. More than 50 million individuals are already affected by this condition, and as we approach the middle of the 21st century, this figure is anticipated to drastically increase (Andrade-Guerrero et al., 2023). Throughout the study, the incidence (147.95%), prevalence (160.84%), and mortality rate (189.29%) of dementia increased significantly. In 2050, it is anticipated that there would be 152.8 million cases worldwide (GBD 2019; Dementia Forecasting Collaborators, 2022; Dos Santos *et al*., 2018).

Several enzymes are involved in the progression of AD; in our study, we focused on acetylcholinesterase (AChE), a major neurotransmitter. Acetylcholine (ACh), a naturally occurring neurotransmitter, is rapidly broken down into acetic acid and choline by hydrolysis. Since the cholinergic deficit in AD was identified, AChE has been extensively studied in the tissues affected by the disease.

In the course of cholinergic transmission, the neurotransmitter AChE is released from nerve fibres. This neurotransmitter sends the message to trigger a response by attaching to certain receptors on other cholinergic nerve fibres. Memory problems have been observed in individuals with AChE inhibitors and have been linked to damage to the cholinergic neurotransmission that produces acetylcholine (Cipriani *et al*., 2011). The cholinesterase enzymes reduce the amount of ACh by hydrolyzing the molecule, especially AChE, which is found in the synaptic cleft of cholinergic neurons (Silman, 2021). These enzymes are bound by cholinesterase inhibitors, which raise the concentration of ACh in the synapses (Stanciu *et al*., 2020). Based on the discovery that disruption of cholinergic pathways in the cerebral cortex and basal forebrain leads to the cognitive impairment of AD patients, AChE inhibitors have been created. Reduced ACh breakdown and subsequent ACh buildup are the effects of AChE inhibition. The increased stimulation of the muscarinic and nicotinic receptors brought on by this additional ACh aids in treating AD's memory issues (Santos *et al*., 2018). AChE inhibitors can penetrate the blood brain barrier (BBB) to varying degrees. Commonly prescribed medications with good BBB penetration for AD include donepezil, rivastigmine, and tacrine.

Corresponding author: Dr. Mohammad Hayatul Islam

IIRC-5, Clinical Biochemistry and Natural Product Research Lab, Department of Biosciences, Faculty of Science Integral University, Lucknow-226010, Uttar Pradesh, India

E-mail: hayatbiotech@gmail.com, hayatbt@iul.ac.in

Tel.: +91-9368134040

In 1996, AD therapy with donepezil was authorized. In addition, rivastigmine has easy permeability to the BBB as it is a small molecule. In the year 2000, it was licensed for the treatment of Parkinson's-related dementia as well as also approved for AD management (Reingold *et al*., 2007). Galantamine was approved for the treatment of mild to moderate AD in February 2001. Tacrine was the first medication authorized in 1993 for the treatment of AD and is a significant AChE and BuChE inhibitor. Later on, it was discontinued as it was causing liver toxicity. These inhibitors cause several toxicities, so there is an urgent need for an inhibitor from natural sources that would be less toxic or nontoxic. In this attempt, a screening of plant derived metabolites was performed to evaluate their druggability and inhibitory effect against AChE a key target of AD.

2. Material and Methods

2.1 Preparation of protein

The protein was retrieved from RCSB database of PDB ID 4M0E and was modified by using discovery studio. The AChE structure was determined by the X-ray diffraction having a resolution of 2Å and zero mutation. The structure is pre-processed before docking by removing the HETATMs, which include water residues, ions, and other small molecules, to prevent steric clashes. All the pre-processing is achieved by using Discovery Studio. The Kollmann charges were applied to the modified structure and later solvated using the AutoDock tool to obtain the final structure of the biological target protein (Sharma *et al*., 2018).

2.2 Preparation of ligand

In our study, we have compiled a library of hundred secondary metabolites that are the result of a comprehensive survey through literature studies. The metabolites that are reported to have neuroprotective properties were incorporated into this study. The structures of these ligands were obtained in sdf format from the PubChem database. The protein structure in PDB format was obtained through Discovery Studio. The ligand was also pre-processed before being subjected to molecular docking studies. Initially, the ligand is energy minimized, followed by optimization by applying partial charges (MMFF94x and gasteiger) and the CHARMM force field. During the energy minimization step, a gradient energy of about 0.001 kcal/mol was used while leaving the other parameters at their default values. Ligand processing was also achieved by utilising the AutoDock tool (Sharma *et al*., 2018).

2.3 Pharmacokinetic analyses

2.3.1 Lipinski's rule of five

The early-stage identification of the small molecules with drug-like characteristics provides greater help in the drug development procedure as it prevents unnecessary expense, time, and *in vitro* analysis in the traditional approach to drug development. The compiled compounds were screened using Lipinski's filters. Using the online software Molinspiration (http://www.molinspiration.com/), we determine whether the compounds are drug-like or not. The attributes of the drug likeness filter include the molecular weight of the molecules (<50 kDa), the number of hydrogen donors (>5) and acceptors (<10), and the logP of the compounds (also known as the partition coefficient, *i.e.* (<5). If, the secondary metabolites fail to follow these parameters or have more than 1 violation, they are regarded as having poor oral bioavailability and hence are removed for further studies (Lipinski *et al*., 2012).

2.3.2 ADME\tox properties

The ADME and toxicity assessment is an important parameter in determining a drug's therapeutic potential against a disease. The compounds that obey the Lipinski criteria are further subjected to ADME and toxicity studies by exploiting the web tool PreADMET server (http://preadmet.bmdrc.org/). This server computes the pharmacokinetic parameters in terms of human intestinal absorption (%HIA should be more than 90%), $CaCO_2$ cell permeability (Pcaco-2 should be between 40 to 70%), Maden Darby canine kidney permeation (PMDCK should be between 25-70%), skin permeability (P_{Skin} between –1.0 to –8.0), plasma protein binding (PPB should be less than 98%), penetration of the BBB (above 1), non-inhibitor for cytochrome CYP2D6 and no computed toxicity, *i.e.*, mutagenicity and carcinogenicity. The secondary metabolites that have computed ADME/tox values within the defined range are filtered for further docking analysis.

2.4 Molecular docking analysis

A molecular docking analysis was conducted with the prepared receptor and ligand by Auto Dock 4.2 to calculate binding affinities and hydrogen bond interactions. The algorithm of the exhaustive search Lamarckian Genetic Algorithm was executed to perform the docking function (to provide the best 10 conformers for each inhibitor molecule) for estimating the free energy of binding and inhibition constant (Ki) (Allouche, 2011). For all targets, the grid was prepared according to the binding pockets of the AChE protein, so that the active site residues are within the grid area while keeping other parameters at default (Sharma *et al*., 2022). The AChE binding site has two subsite one that contains a catalytic triad of SER203, GLU334 and HIS447 residues. While, the second anionic catalytic site (choline-binding region) is responsible for the AChE breakdown into choline and acetate within the esteratic subsite. The metabolites were subjected to screening based on their free binding energy, Ki, involvement of interaction residues, and hydrogen bonds (Morris *et al*., 2009). In order to determine the ligand configurations and positions generated by the molecular docking, redocking studies were used to confirm the docking methodology and variables. This may offer the plausible and legitimate way of possible binding between the co-crystal ligand and the target protein. Consequently, on the native protein, the capacity of the ADT to duplicate each ligand's location and orientation in a manner comparable to that of the co-crystal ligand was assessed. The crystal structure with the lowest RMSD value was taken into consideration for further analysis. The best docked findings were utilized to construct the structure with the highest binding affinity using Pymol and the Discovery Studio Visualizer 3.5 (Sharma *et al*., 2018).

2.5 Molecular dynamics simulation (MDS)

The complex with the best binding affinity against the AChE protein is further evaluated for its stability using the MDS study. The investigation was done by the Groningen Machine for Chemical Simulations (GROMACS 5.1 package) (Abraham *et al*., 2015). To begin the simulation study, the all-atom CHARMM force field must be used to generate the topology of both the receptors and the

ligands. The all-atom CHARMM-27 force field from GROMACS is used to create the receptor protein topology files, whereas the SwissParam online server tool is used to create the ligand topology files (Zoete *et al*., 2011). A 3.0-nm separation of water model points (TIP3P) which were constructed from the target protein to the box's faces, was established to maintain the MDS under the conditions of a periodic boundary (Price *et al*., 2004). To prevent collisions between protein molecules, SPC water molecules were used in a dodecahedral model box with exterior edges and a margin of 10 Å (Glättli *et al*., 2002). In order to maintain the maximum force less than 1000 kj/mol/nm, the solvated system is neutralized by sodium ions in every simulation technique, and the steric conflicts of the system are avoided by executing the steepest energy minimization of roughly two thousand steps. Particle Mesh Ewald (PME) was exploited to compute the electrostatic interaction at larger distances, and the bond length was constrained utilizing the LINCS (linear constraint solver) algorithm (Darden *et al*., 1993). The non-bonded Van der Waals interaction is calculated at a threshold of around 1.0 nm (Hess *et al*., 1997). Moreover, the system is calibrated at 300 K under NVT and NPT for 1000 picoseconds (ps) at a pressure of 1 bar (constant particle number, volume, and temperature). Using a velocity-rescaling thermostat, 300 K of temperature coupling was attained with a constant time of 0.1 ps (Bussi *et al*., 2007). The Parrinello-Rahman barostat's given approach was used at a constant time of 1 ps to determine the 1 bar pressure (Parrinello and Rahman, 1981). The protein-ligand system was then put through a 100 ns dynamic simulation. Every two femtoseconds (fs) at each phase, a leap-frog integrator was employed, and the dynamic results' coordinates were stored for further analysis. Using the GROMACS gmx modules, the analysis of RMS, RMSF, gyrate, H-bond, and SASA was assessed. The MDS graphs were plotted using the XMgrace tool.

2.6 MMPBSA and per-residue contribution

The free binding energy of the complex system, *i.e.*, between the AChE protein and the active molecules is determined by exploring the MM-PBSA (Molecular Mechanics-Poisson-Boltzmann Surface Area) methodology (Kumari *et al*., 2014). MM-PBSA that is used to assess the binding free energy ("Gbind) is computed by using the below mentioned equations:

$$\Delta G_{bind} = T\Delta S \approx \Delta E_{mm} + \Delta G_{solv} - T\Delta S$$

$$\Delta E_{mm} = \Delta E_{int} + \Delta E_{elec} - \Delta E_{vDw}$$

$$\Delta G_{solv} = \Delta Gelec_{solv} + \Delta GvDw_{solv}$$

The TΔS represents the entropy contribution of the system along with the energy of the total gas phase, as demonstrated by the ΔE_{mm}. Similarly, the free solvation energy is represented by ΔG_{solv}. To compute the component of the electrostatic energy of a solvation in a continuum solvent, the Poisson-Boltzmann method is employed. The non-polar solvation energy may be exploited to estimate the solvent-accessible surface area (Lee and Olson, 2013). The energy contribution of amino acid residues within 5Å of the ACHE active site was calculated by analyzing the decomposition of each residue. The assessment of energy contribution per residue helps in understanding the interactions between the inhibitor molecules and the proteins, along with their backbone atoms and side chains. The residues involved in the catalytic triad of AChE subsite and the active pocket containing residues (TYR124, SER125, SER203, TRP286, SER293, VAL294, PHE295, PHE297, TYR337, PHE338, TYR341 and HIS447) were assessed for this analysis.

3. Results

3.1 Study of pharmacokinetic properties and drug likeness

The potential of a drug to penetrate or be absorbed by the human body across the bilayer of phospholipid was evaluated by the Lipinski attributes, which also affirm the oral bioavailability of the molecules. In this study, we have compiled 100 compounds that were subjected to drug likeness analysis and screened on the basis of fulfilling the parameters of Lipinski's rule of five by using the online software molinspiration. Among all 100 compiled compounds, only 40 compounds fulfilled the drug likeness parameters, with a total of zero violations. The compounds obeying the rule of five are considered to have high bioavailability with significant oral absorption potential. The screened compounds with zero n-violation (*i.e.*, 40) were filtered and subjected to ADME/Tox assessment with an online software program called PreADME/Toxicity.

On the basis of this pharmacokinetic study, only 4 compounds out of 40 fulfilled all the descriptors of ADME/Tox. All four of the selected compounds have high HIA, MDCK, and Caco-2 absorption with selective skin permeation along with high BBB and PPB distribution, making them good agents against neuro-targeting. The selected candidates also showed non-inhibitory properties against CYP2D6. Furthermore, no toxicity is predicted for the compounds kanzonol R and racemosol. However, the compounds sabinene and quindoline were shown to be mutagenic but not carcinogenic in animal models. Hence, these four compounds were subjected to docking analysis to determine the best potent inhibitor for the AChE protein (Table 1).

Table 1: ADME/Tox properties of selected compounds and standard drugs

S.No.	Compound name	Toxicity		Absorption				Distribution		Metabolism
		Mutagenicity	Carcinogenicity	HIA[a]	CaCo-2[b]	MDCK[c]	P_{Skin}[d]	PPB[e]	BBB[f]	CYP2D6[g]
1.	Quindoline	Mutagen	Non-carcinogen	98.99	41.34	226.7	-3.098	87.82	1.434	Non
2.	Racemosol	Non-mutagen	Non-carcinogen	93.57	40.88	125.63	-2.584	100.0	3.200	Non
3.	Sabinene	Mutagen	Non-carcinogen	100.0	23.49	300.5	-1.367	60.97	5.756	Non
4.	Kanzonol R	Non-mutagen	Non-carcinogen	93.97	33.04	O.046	-2.676	99.82	3.127	Non

[a] Percentage of human intestinal absorption, [b] Cell permeability (CaCo-2 in nm/sec), [c] Cell permeability Maden Darby Canine Kidney in nm/sec, [d] Skin permeability (nm/sec), [e] Percentage of plasma protein binding, [f] Blood Brain Barrier (CBrain/CBlood), [g] Cytochrome P450 2D6 binding.

3.2 Molecular docking analysis

The molecular docking results are summarized in Table 2. All the selected compounds docked with the target AChE. Kanzonol R showed the best binding affinity with a binding energy of -10.67 kcal/mol with the AChE protein target as compared to other compounds and the redock co-crystal ligand (NAG). The native co-crystal ligand has an interaction energy of about –6.46 kcal/mol with 18.38 uM of Ki. The residues involve in the interaction between the NAG and the AChE protein includes SER203, PHE338, and HIS447. The compounds quindoline and racemosol also have a binding energy higher than the native ligand (NAG) but higher Ki value. While sabinene shows the lowest binding potential as compare to the other inhibitor molecules and the NAG (Table 2). The interaction residues of each complex were evaluated, and the analysis showed that all the inhibitor molecules interacted with the same residues of the AChE as with the NAG-AChE interaction pocket (Figure 1 a and c). The docking analysis demonstrated that kanzonol R has a significant binding potential, as evidenced by its interaction with similar residues in the binding pocket of AChE as the redock ligand (TRP286, LEU289, GLU292, SER293, VAL294, PHE295, ARG296, PHE297, PHE338 and TYR341). In addition, kanzonol R also exhibited two similar hydrogen bonds (with TYR341 and PHE295) as the redock conformation (Figures 1 b and d).

Table 2: Results of molecular mocking analysis binding energy, inhibition constant and interactive amino acids

S.No.	Compounds	Binding energy (kcal/mol)	Ki (µM)	Interacting amino acid	Amino acids involve in hydrogen bond formation
1.	Redock (NAG)	-6.46	18.38	TRP286, LEU289, GLU292, SER293, VAL294, PHE295, ARG296, PHE297, PHE338 and TYR341	TYR341, ARG296, SER293 and PHE295
2.	Quindoline	-8.59	508.94	GLN71, TYR72, VAL73, ASP74, TRP86, ASN87, PRO88, GLY120, GLY121, TYR124, SER125, GLY126, TYR133, GLU202 and TYR337	TYR337
3.	Racemosol	-8.69	423.70	TYR72, TYR124, TRP286, LEU289, SER293, VAL294, PHE295, ARG296, PHE297, TYR337, PHE338 and TYR341	PHE295
4.	Sabinene	-5.83	53.37	TRP286, SER293, VAL294, PHE295, ARG296, PHE297, PHE338 and TYR341	None
5.	Kanzonol R	-10.67	73.88	TYR124, SER125, SER203, TRP286, SER293, VAL294, PHE295, PHE297, TYR337, PHE338, TYR341 and HIS447	TYR124, PHE295, TYR337 and TYR341

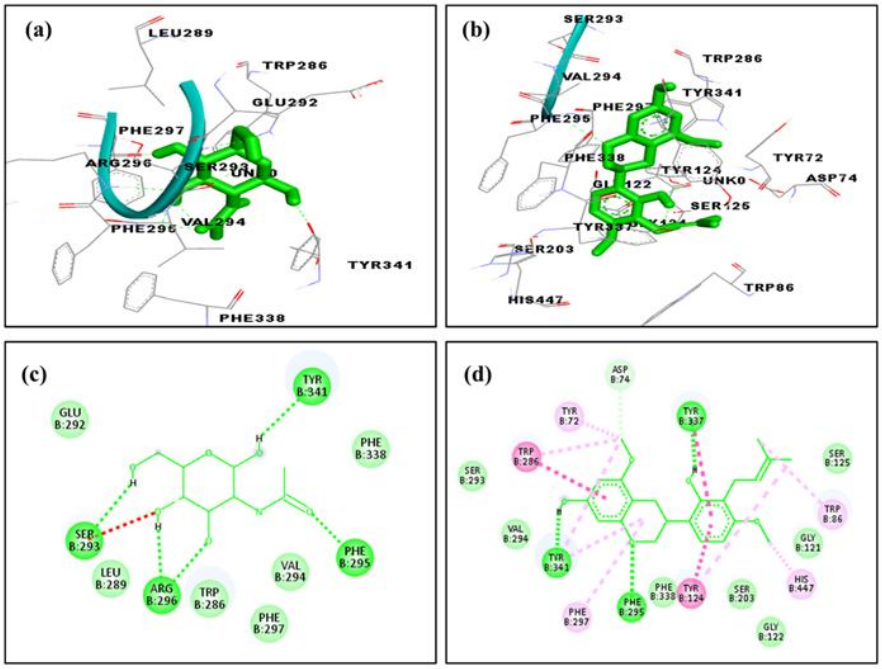

Figure 1: The 3D and 2D structure of the best docked conformer of the redock (NAG) ligand (a) and (c) and the Kanzonol R (b) and (d) with the AChE protein.

3.3 MD simulation

We conducted a 100-ns MD simulation to comprehend the stability of the complex system as well as the dynamics of the binding complex of the bioactive compound (kanzonol R) and the AChE protein. A change in the protein's conformation also occurs during simulation when the ligand molecules are bound to the active sites of the protein. The trajectories generated from the simulation results were utilized to compute the RMSD (root mean square deviation) and RMSF (root mean square fluctuation) of the backbone along with the protein's radius of gyration (Rg) to evaluate the structural deviation of the system and the changes in the compactness of the protein during the simulation. The computed average RMSD of the redock-cocrystal ligand (NAG) with the AChE protein was about 0.164 ± 0.015 nm, while for the system containing the inhibitor compound (kanzonol R), it was about 0.154 ± 0.016 nm) The NAG-AChE system shows an increased structural deviation until 30 ns, followed by constant RMSD values showing a convergence in the RMSD plot, representing a system reaching equilibrium. Similarly, the bioactive compound and protein system (kanzonol-AChE) also has an increased fluctuation in the RMSD value until 35 ns, after which the system converges to equilibrium. The RMSD plot shows that the kanzonol-ACHE trajectories are comparatively more stable than the NAG-AChE trajectories during the 100-ns run, as they have comparatively less fluctuation in the deviation (Figure 2 a). The RMSF plot suggested a magnitude of fluctuation in the residues of AChE proteins upon the binding of the active compound. The RMSF plot demonstrated that the binding of the inhibitor ligand (NAG) causes an increase in the residual fluctuation as compared to the co-crystal ligand interaction with the AChE (Figure 2 b). The increased fluctuation in the RMSF plot represents the inhibitor compound (kanzonol R) having an increased flexibility after binding with protein, which also confirms the system's stability.

Furthermore, the compactness of the protein after the binding of the ligand molecules is also evaluated using the parameter of radius of gyration (Rg) for the 100 ns trajectories. The co-crystal ligand (NAG) and kanzonol R have an average Rg value of about 2.327 ± 0.007 nm and 2.325 ± 0.006 nm, respectively. The averages for both trajectories were computed to be almost equal. The Rg values of the NAG trajectories showed a rise in the deviation till 15 ns, representing the loose packing of the protein, followed by a slight rise and constant deviation value of Rg till 80 ns, which further declined after 90 ns. However, the inhibitor system showed a fluctuation in the Rg values until 30 ns, after which it maintained the constant deviation in the Rg values until 100 ns (Figure 2 c). The Rg plots showed that kanzonol R had a stable, compact, and tightly bound behavior of the protein structure during the 100 ns simulation as compared to the NAG trajectories.

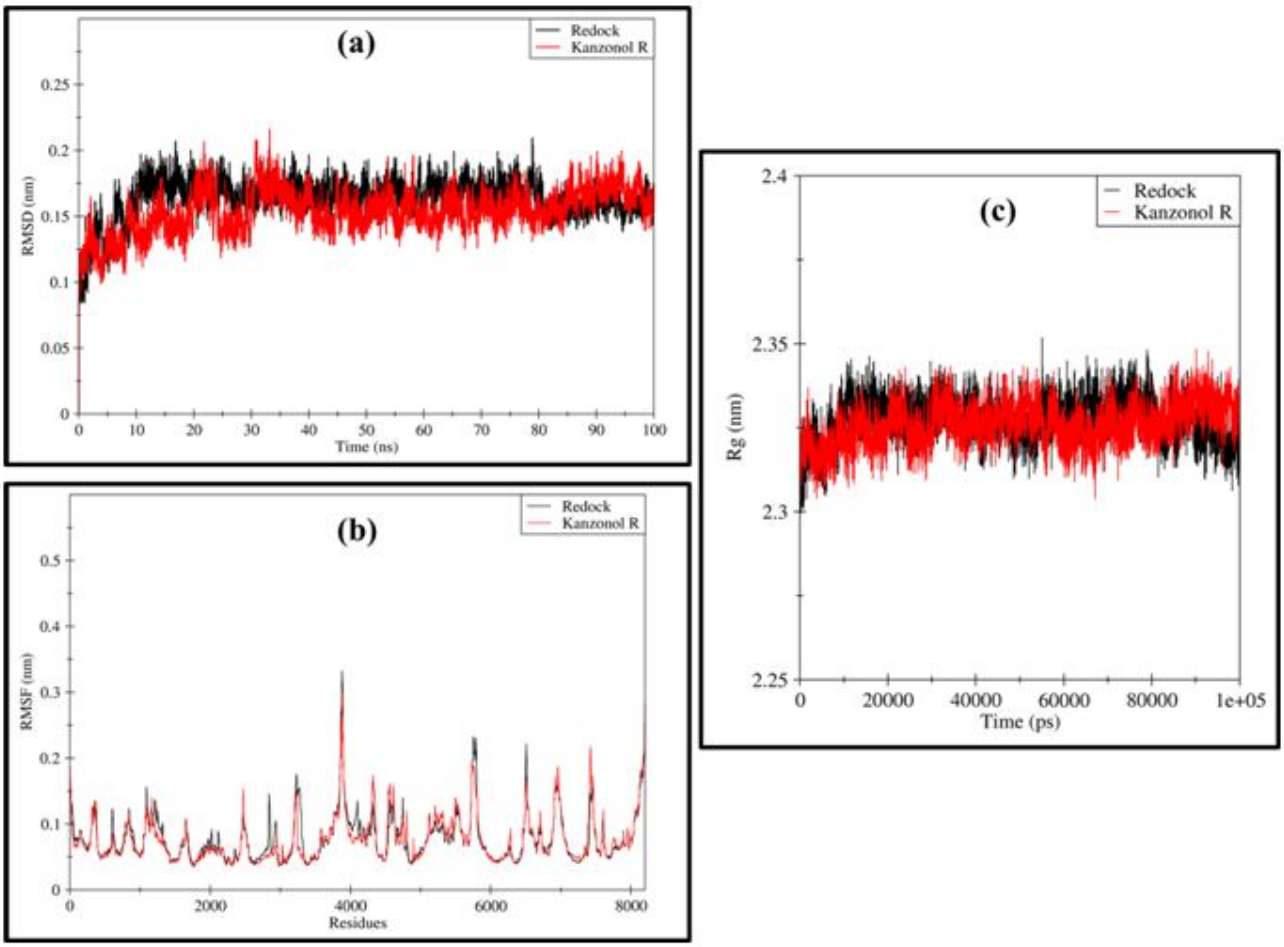

Figure 2: The plot representation of (a) RMSD, (b) RMSF and (c) Rg (radius of gyration) of the redock (NAG) ligand and kanzonol R complex system with AChE protein (NAG system represented with black and kanzonol R with red color).

3.4 MM-PBSA and residue contribution

The algorithm of molecular mechanics in MM-PBSA was employed to predict the binding free energies in order to determine the stability of the interactions between the bioactive molecules and the AChE protein. The MM-PBSA algorithm generates the energies in terms of van der Waals, polar solvation, electrostatics, and SASA, whose summation provides the total interaction energy involved in the complex formation. Our selected ligand kanzonol R as compare to the NAG shows the best interaction potential with the AChE protein, as it has the lowest total binding energy (–195.284 ± 16.391 kJ/mol). For both complex systems, van der Waals and electrostatic interactions contribute the most energy to complex formation.

Table 3: Involvement of various energy parameters in the formation of the complex with protein AChE and ligands (NAG and kanzonol R)

MM-PBSA energy parameters (kJ/mol)	Co-crystal ligand (NAG)	Kanzonol R
Total binding energy	-124.711 ± 16.290	-195.284 ± 16.391
Van der Waals	-111.218 ± 9.048	-207.967 ± 12.809
Electrostatic	-119.977 ± 23.551	-69.743 ± 20.336
Polar solvation	118.696 ± 14.921	104.735 ± 17.804
SASA	-12.212 ± 0.784	-22.308 ± 0.958

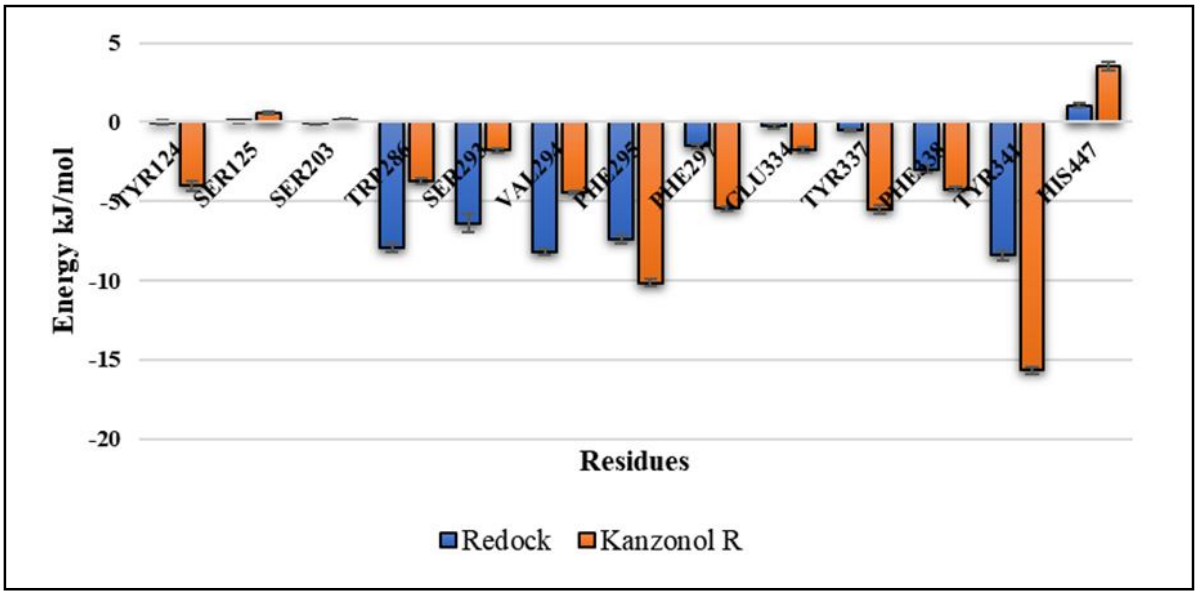

Figure 3: Bar graph representation of per-residue in energy contribution for NAG and kanzonol R system.

The involvement of the residues SER203, GLU334 and HIS447 in complex formation was also investigated using residue decomposition. The NAG and AChE interaction system trajectories show the favorable interaction of residues SER203 (– 0.077 kcal/mol) and GLU334 (– 0.262 kcal/mol). While for kanzonol R, the residue GLU334 (–1.7598 kcal/mol) shows a favorable energy contribution in the binding to the protein target. Furthermore, the residues TYR341 (–15.65 kJ/mol) and PHE295 (–10.15 kJ/mol) have the most favorable involvement in the kanzonol-AChE system's energy contribution. While, for the redock co-crystal system, TYR341 (– 8.39 kJ/mol), VAL294 (-8.166 kJ/mol), TRP286 (–7.919 kJ/mol), and PHE295 (– 7.38 kJ/mol) have the most significant and favorable contributions (Figure 3).

4. Discussion

When there is an interruption in the signaling among synapsis, this result in the excess production of the neurotransmitter named AChE (plays important role in the neurodegenerative disease called AD) which is the major concern of our study. As a result, secondary metabolites are extensively studied due to their no or less toxic against human responses.

Most of the drugs failed due to poor pharmacokinetic analysis, In this context we screened out the bioactive metabolites for their pharmacokinetic properties. Furthermore, selected compounds were anlyzed for their binding affinity against the ke target of AD by molecular docking approch. computational method, molecular docking, is widely used to elucidate the mechanism of action and rationalize structure activity relationships of natural products.

The aim of docking is to accurately predict the positioning of a ligand within a protein binding pocket and to estimate the strength of the binding with a docking score (Allahbi and Singh, 2022). Computational methods also provide the means to discover previously undescribed binding sites on known protein structures. Pocket finders detect solvent-accessible cavities in the protein surface that can indicate potential ligand binding sites.

Among the the selected metabolites (Table 2) kanzonol R exhibited significant binding affinity in the active site of AChE. Kanzonol R is a flavonoid compound in a class of organic compounds having 5-O-methylated iso-flavonoids. This compound is reported to have been isolated from the *Glycyrrhiza glabra* L. (licorice) plant (Hussain *et al*., 2014; Batiha *et al*., 2020; Irani *et al*., 2020). Licorice has been extensively studied for its chemical composition and pharmacological activities (such as cytotoxic activity, antioxidant potential, anti-inflammatory, anticancer, antimicrobial, and many more) owing to the presence of a wide spectrum of bioactive compounds, including kanzonol R (Sharma *et al*., 2017; Nomura *et al*., 2002). However, the compound kanzonol R has not yet been evaluated against neurodegenerative diseases. AD is a neurological disorder (Sekeroglu and Gezici, 2019). Hence, this study gives an insight into the probability that this isoflavonoid will be an effective agent for targeting neurodegenerative diseases after its further *in vitro* and *in vivo* validation. Among the selected four secondary metabolite, kanzonol R ranked best in all computational analysis done in our study. Furthermore, our study revealed that kanzonol R can be a powerful deterrent of our targeted protein AChE and aids in the development of new Alzheimer's drug.

5. Conclusion

Compounds that will inhibit the enzyme AChE in AD brain are potential therapeutic agents. On the basis of the pharmacokinetic study, kanzonol R was found to fulfil all the tested descriptors for both duggability and ADME/Tox. Furthermore, molecular docking results indicated that kanzonol R binds significantly in the conserved sites of AChE and exhibits stable dynamic behavior over a 100-ns trajectory. Thus, it is worth carrying out further investigations into its neuroprotective properties both *in vitro* and *in vivo* to optimize it as an anti-neurodegenerative agent to treat conditions like AD.

Acknowledgments

The authors acknowledge the office of Doctoral Studies and Research for critically reviewing the manuscript and providing the manuscript number (IU/R&D/2023-MCN0001886).

Conflict of interest

The authors declare no conflicts of interest relevant to this article.

References

Abraham, M. J.; Murtola, T.; Schulz, R.; Páll, S.; Smith, J. C.; Hess, B. and Lindah, E. (2015). Gromacs: High performance molecular simulations through multi-level parallelism from laptops to supercomputers. SoftwareX., **1**(2):19-25. DOI:https://doi.org/10.1016/j.softx.2015.06.001

Allahabi, Z. and Singh, S. (2022). In silico approach for discovery of drug against the peroxisome proliferator-activated receptor gamma for diabetes treatment. Ann. Phytomed., **11***(1):299-310.* DOI:http://dx.doi.org/10.54085/ap.2022.11.1.31

Allouche, A. R. (2011). Software news and updates gabedit-A graphical user interface for computational Chemistry softwares. J. Comput. Chem., **32**:174-182. DOI:10.1002/jcc.21600

Andrade-Guerrero, J.; Santiago-Balmaseda, A.; Jeronimo-Aguilar, P.; Vargas-Rodríguez, I.; Cadena-Suárez, A.R.; Sánchez-Garibay, C.; Pozo-Molina, G.; Méndez-Catalá, C.F.; Cardenas-Aguayo, M.D.C.; Diaz-Cintra, S. and Pacheco-Herrero, M. (2023). Alzheimer's disease: An updated overview of its genetics. Int. J. Mol. Sci., **24**(4):3754. DOI:10.3390/ijms24043754

Batiha, G.E.; Beshbishy, A.M.; El-Mleeh, A.; M. Abdel-Daim, M. and Devkota, H. P. (2020). Traditional uses, bioactive chemical constituents, and pharmacological and toxicological activities of *Glycyrrhiza glabra* L. (Fabaceae). Biomolecules., **10**:352. DOI: 10.3390/biom10030352.

Bussi, G.; Donadio, D. and Parrinello, M. (2007). Canonical sampling through velocity rescaling. J. Chem. Phys., **126**:014101. DOI:https://doi.org/10.1063/1.2408420.

Cipriani , G.; Dolciotti, C.; Picchi, L. and Bonuccelli, U. (2011). Alzheimer and his disease: A brief history. Neurol. Sci., **32**(2):275-9. DOI: 10.1007/s10072-010-0454-7.

Darden, T.; York, D. and Pedersen, L. (1993). Particle mesh Ewald: An Nlog(N) method for Ewald sums in large systems. J. Chem. Phys., **98**:10089-10092. DOI:https://doi.org/10.1063/1.464397.

Davenport, F.; Gallacher, J.; Kourtzi, Z.; Koychev, I.; Matthews, P.M.; Oxtoby, N.P.; Parkes, L.M.; Priesemann, V.; Rowe, J.B.; Smye, S.W. and Zetterberg, H. (2023). Neurodegenerative disease of the brain: A survey of interdisciplinary approaches. J. R. Soc. Interface., **20**(198):20220406. DOI: https://doi.org/10.1098/rsif.2022.0406.

Glättli, A.; Daura, X. and Van Gunsteren, W. F. (2002). Derivation of an improved simple point charge model for liquid water: SPC/A and SPC/L. J. Chem. Phys., **116**:9811-9828. DOI:https://doi.org/10.1063/1.1476316.

Hess, B.; Bekker, H.; Berendsen, H. J. C. and Fraaije, J. G. E. M. (1997). LINCS: A linear constraint solver for molecular simulations. J. Comput. Chem., **18**:1463-1472. DOI:https://doi.org/10.1002/(SICI)1096-987X(199709)18:12<1463::AID-JCC4>3.0.CO;2-H.

Huang, Y.; Dou, K.; Zhong, X.; Shen, X.; Chen, S.; Li, H.; Chen, L.; Cui, M.; Dong, Q.; Tan, L. and Yu, J. (2020). Pharmacological treatment of neuropsychiatric symptoms of dementia: A network meta-analysis protocol. Ann. Transl. Med., **8**(12):746. DOI: 10.21037/atm-20-611.

Hussain, K.; Khalid, S.; Iram, N. and Ali, M. A. (2014). A review: Medicinal Importance of *Glycyrrhiza glabra* L. (Fabaceae Family). Glob. J. Pharmacol., **8**(1):08-13. DOI:10.5829/idosi.gjp. 2014.8.1.81179.

Irani, M.; Sarmadi, M.; Bernard, F.; pour, G. H. E. and Bazarnov, H.S. (2010). Leaves antimicrobial activity of *Glycyrrhiza glabra* L. Iran. J. Pharm. Res., **9**(4):425-428. PMC3870067

Kumari, R.; Kumar, R. and Lynn, A. (2014). G-mmpbsa-A GROMACS tool for high-throughput MM-PBSA calculations. J. Chem. Inf. Model., **54**:1951-1962. DOI:https://doi.org/10.1021/ci500020m.

Lee, M. S. and Olson, M. A. (2013). Comparison of volume and surface area nonpolar solvation free energy terms for implicit solvent simulations. J. Chem. Phys., **139**(4):044119 DOI:https://doi.org/10.1063/1.4816641.

Lipinski, C. A.; Lombardo, F.; Dominy, B. W. and Feeney, P. J. (2012). Experimental and computational approaches to estimate solubility and permeability in drug discovery and development settings. Adv. Drug Deliv. Rev., **64**:4-17. DOI:https://doi.org/10.1016/j.addr.2012.09.019.

Marucci, G.; Buccioni, M.; Ben, D. D.; Lambertucci, C.; Volpini, R. and Amenta, F. (2021). Efficacy of acetylcholinesterase inhibitors in Alzheimer's disease. Neuropharmacology, **9**(11):1689. DOI: 10.1016/j.neuropharm.2020.108352.

Morris, G. M.; Ruth, H.; Lindstrom, W.; Sanner, M. F.; Belew, R. K.; Goodsell, D. S. and Olson, A. J. (2009). Software news and updates AutoDock4 and AutoDockTools4: Automated docking with selective receptor flexibility. J. Comput. Chem., **30**:2785-2791. DOI:https://doi.org/10.1002/jcc.21256.

Nomura, T.; Fukai, T. and Akiyama, T. (2002). Chemistry of phenolic compounds of licorice (Glycyrrhiza species) and their estrogenic and cytotoxic activities. Pure. Appl. Chem., **74**:1199-1206. DOI:https://doi.org/10.1351/pac200274071199.

Parrinello, M. and Rahman, A. (1981). Polymorphic transitions in single crystals: A new molecular dynamics method. J. Appl. Phys., **52**:7182-7190. DOI:https://doi.org/10.1063/1.328693.

Poddar, M. K.; Banerjee, S.; Chakraborty, A. and Dutta, D. (2021). Metabolic disorder in alzheimer's disease. Metab. Brain. Dis. **36**(5):781-813. DOI: 10.1007/s11011-021-00673-z.

Price, D. J. and Brooks, C. L. (2004). A modified TIP3P water potential for simulation with Ewald summation. J. Chem. Phys., **121**:10096-10103. DOI:https://doi.org/10.1063/1.1808117.

Reingold, J.L.; Morgan, J.C. and Sethi, K.D. (2007). Rivastigmine for the treatment of dementia associated with Parkinson's disease. Neuropsychiatr. Dis., Treat., **3**(6):775-783. DOI: 10.2147/ndt.s1134.

Sharma, V.; Katiyar, A. and Agrawal, R. C. (2017). Glycyrrhiza glabra: Chemistry and pharmacological activity. Sweeteners, **31**:87-100. DOI: 10.1007/978-3-319-27027-2_21

Santos, T. C. D.; Gomes ,T. M.; Pinto1, B. A. S.; Camara, A. L. and Paes, A. M. D. A. (2018). Naturally occurring acetylcholinesterase inhibitors and their potential use for Alzheimer's disease therapy. Front. Pharmacol., **9**:1192. DOI:https://doi.org/10.3389/fphar.2018.01192.

Sekeroglu, N. and Gezici, S. (2019). Astragalus neurocarpus Bioss. as a potential source of natural enzyme inhibitor associated with Alzheimer's and Parkinson diseases along with its rich polyphenolic content and antioxidant activities. Ann. Phytomed., **8**(1):82-87. DOI:http://dx.doi.org/10.21276/ap.2019.8.1.9.

Sharma, M.; Sharma, N.; Muddassir, M.; Rahman, Q. I.; Dwivedi, U. N. and Akhtar, S. (2022). Structure-based pharmacophore modeling, virtual screening and simulation studies for the identification of potent anticancerous phytochemical lead targeting cyclin-dependent kinase 2. J. Biomol. Struct. Dyn., **40**: 9815-9832. DOI:https://doi.org/10.1080/07391102.2021.1936178.

Sharma, A.; Islam, M. H.; Fatima, N.; Upadhyay, T. K.; Khan, M. K. A.; Dwivedi, U. N. and Sharma, R. (2018). Deciphering the binding of natural terpenoids to *Mycobacterium tuberculosis* type III polyketide Synthase18 (PKS18): An *in silico* approach. J. Appl. Pharm. Sci., **8**(5):026-034. DOI: 10.7324/JAPS.2018.8504.

Silman, S. (2021). The multiple biological roles of the cholinesterases.Prog. Biophys. Mol. Biol., **162**:41-56. DOI:10.1016/j.pbiomolbio.2020.12.001.

Stanciu, G. D.; Luca, A.; Rusu, R. N.; Bild, V.; Chiriac, S. L. B.; Solcan, C.; Bild, W. and Ababei, D.C. (2020). Alzheimer's disease pharmacotherapy in relation to cholinergic system involvement. Biomolecules, **10**(1):40. DOI:10.3390/biom10010040.

Yamamoto, M.; Kanamoto, T.; Terakubo, S.; Nakashima, H.; Uesawa, Y.; Kagaya, H. and Sakagami, H. (2016). Antiviral and antitumor activity of licorice root extracts. *In vivo*., **30**(6):777-785. DOI:10.21873/invivo.10994.

Zoete, V.; Cuendet M. A.; Grosdidier, A. and Michielin. (2011). Swiss param: A fast force field generation tool for small organic molecules. J. Comput. Chem., **32**(11):2359-68. DOI:10.1002/jcc.21816.

Citation **Firdaus Jahan, Akanksha Sharma and Mohammad Hayatul Islam (2023). PComputational identification of bioactive compound with neuroprotective potential for the management of Alzheimer's disease by targeting AChE protein. Ann. Phytomed., 12(1):269-276. http://dx.doi.org/10.54085/ap.2023.12.1.2.**